JNCI J Natl Cancer Inst (2018) 110(1): djx123

doi: 10.1093/jnci/djx123
First published online August 25, 2017
Article

ARTICLE

Comprehensive Intrametastatic Immune Quantification and Major Impact of Immunoscore on Survival

Bernhard Mlecnik*, Marc Van den Eynde*, Gabriela Bindea*, Sarah E. Church, Angela Vasaturo, Tessa Fredriksen, Lucie Lafontaine, Nacilla Haicheur, Florence Marliot, Daphné Debetancourt, Géraldine Pairet, Anne Jouret-Mourin, Jean-Francois Gigot, Catherine Hubert, Etienne Danse, Cristina Dragean, Javier Carrasco, Yves Humblet, Viia Valge-Archer, Anne Berger, Jérôme Galon

Affiliations of authors: Laboratory of Integrative Cancer Immunology, INSERM, UMRS1138, Paris, France (BM, MVdE, GB, SEC, AV, TF, LL, FM, AB, JG); Université Paris Descartes, Sorbonne Paris Cité, UMRS1138, Paris, France (BM, MVdE, GB, SEC, AV, TF, LL, FM, AB, JG); Sorbonne Universités, UPMC Univ Paris 06, UMRS1138, Centre de Recherche des Cordeliers, Paris, France (BM, MVdE, GB, SEC, AV, TF, LL, FM, AB, JG); Inovarion, Paris, France (BM); Department of Medical Oncology, Cliniques Universitaires St-Luc and Institut de Recherche Clinique et Experimentale (Pole MIRO), Institut Roi Albert II, Université Catholique de Louvain, Brussels, Belgium (MVdE, DD, GP, AJM, JFG, CH, ED, CD, YH); Department of Immunology, HEGP, Assistance Publique-Hopitaux de Paris, Paris, France (NH, FM); AstraZeneca, Cambridge, UK (VVA); Departments of General and Digestive Surgery, HEGP, AP-HP, Assistance Publique-Hopitaux de Paris, Paris, France (AB); Grand Hopital de Charleroi, Charleroi, Belgium (JC)

See the Notes section for the full list of authors and affiliations.
*Authors contributed equally to this work.
Correspondence to: Jérôme Galon, Laboratory of Integrative Cancer Immunology, INSERM UMRS1138, Cordeliers Research Center, 15 rue de l'Ecole de Medecine, 75006, Paris, France (e-mail: jerome.galon@crc.jussieu.fr).

Abstract

Background: This study assesses how the metastatic immune landscape is impacting the response to treatment and the outcome of colorectal cancer (CRC) patients.
Methods: Complete curative resection of metastases (n = 441) was performed for two patient cohorts (n = 153). Immune densities were quantified in the center and invasive margin of all metastases. Immunoscore and T and B cell (TB) score were analyzed in relation to radiological and pathological responses and patient's disease-free (DFS) and overall survival (OS) using multivariable Cox proportional hazards models. All statistical tests were two-sided.
Results: The spatial distribution of immune cells within metastases was nonuniform. Patients, as well as metastases of the same patient, had variable immune infiltrates and response to therapy. A beneficial response was statistically significantly associated with increased immune densities. Among all metastases, Immunoscore (I) and TB score evaluated in the least immune-infiltrated metastases were the strongest predictors for DFS and OS (five-year follow-up, Immunoscore: I 3–4: DFS rate = 27.9%, 95% CI = 15.2 to 51.3; vs I 0–1–2: DFS rate = 12.3%, 95% CI = 4.9 to 30.6; HR = 0.45, 95% CI = 0.28 to 0.70, $P = .02$; I 3–4: OS rate = 64.6%, 95% CI = 46.6 to 89.6; vs I 0–1–2: OS rate = 32.5%, 95% CI = 17.2 to 61.4; HR = 0.32, 95% CI = 0.15 to 0.66, $P = .001$, C-index = 65.9%; five-year follow-up, TB score: TB 3–4: DFS rate = 25.7%, 95% CI = 14.2 to 46.6; vs TB 0–1–2: DFS rate = 5.0%, 95% CI = 0.8 to 32.4; HR = 0.36, 95% CI = 0.22 to 0.57, $P < .001$; TB 3–4: OS rate = 63.7%, 95% CI = 46.4 to 87.5; vs TB 0–1–2: OS rate: 21.4%, 95% CI = 9.2 to 49.8; HR = 0.25, 95% CI = 0.12 to 0.51, $P < .001$, C-index = 67.8%). High TB score and Immunoscore patients had a median survival of 70.5 months, while low patients survived only 25.1 to 38.3 months. Nonresponding patients

Received: October 26, 2016; **Revised:** April 19, 2017; **Accepted:** May 24, 2017

with high-immune infiltrates had prolonged DFS (HR = 0.28, 95% CI = 0.15 to 0.52, P = .001) and OS (HR = 0.25, 95% CI = 0.1 to 0.62, P = .001). The immune parameters remained the only statistically significant prognostic factor associated with DFS and OS in multivariable analysis (P < .001), while response to treatment was not.

Conclusions: Response to treatment and prolonged survival of metastatic CRC patients were statistically significantly associated with high-immune densities quantified into the least immune-infiltrated metastasis.

Considerable progress has been made in the management of metastatic colorectal cancer (CRC). Resection of CRC metastases, surgical techniques, and systemic treatments offer potential for long-term complete remission (1–3). Even with optimal treatment, the risk of metastatic recurrence and subsequent mortality is high. Tumor prognostic and recurrence risk factors like the tumor regression grade have been proposed (4–8).

We previously reported the major role of cytotoxic and memory T cells within primary CRC tumors in predicting the survival of patients (9–12), including those with early-stage cancer (13). The Immunoscore is a standardized scoring system based on densities of two lymphocyte populations infiltrating the core (CT) and invasive margin (IM) of the tumor that has a highly statistically significant prognostic value (14–17). In non-metastatic CRC, time to recurrence and overall survival could be largely governed by the adaptive immune reaction (10,12). In metastases, which are often considered the consequence of a tumor immune evasion, high-Immunoscore within brain metastasis correlated with prolonged survival (14).

Even if multiple data support the introduction of immune cell quantification in colorectal cancer classification, the impact of immune infiltration within metastasis remains an open question (18). Herein, we performed a complete quantification of immune cells within all metastases of patients with complete curatively metastatic resection. Whole slide metastasis sections were thoroughly quantified for CD3+, CD8+, CD45RO+, FOXP3+, and CD20+ cells. The Immunoscore (CD3/CD8) and T and B cell (TB) score (CD8/CD20) were calculated and investigated in relation to clinical and pathological characteristics of the patients and outcome.

Methods

Patients

Records of 153 metastatic CRC patients who underwent complete curative resection of all synchronous and/or metachronous metastases (n = 441) with or without preoperative treatment at the Cliniques Universitaires St-Luc (Brussels, Belgium) between 2004 and 2010 were reviewed. Cohort 1 (114 patients, 338 metastases) and the validation cohort (39 patients, 103 metastases) were obtained in an unbiased manner (Tables 1; Supplementary Table 1, available online). Approval for this research was obtained from the ethic committees of the Cliniques Universitaires St-Luc.

Characterization of Tumor Response to Preoperative Treatment

The radiological response of metastases to preoperative treatment was assessed according to the RECIST 1.1 criteria (19). Complete and partial responses (CR-PRs) were considered a global response, and stable and progressive disease (SD-PD) a non-response. Tumor regression grade (TRG) was assessed according the Rubbia-Brandt classification (TRG 1–2–3 = response; TRG 4–5 = no response) (7).

Table 1. Metastases' characteristics

Characteristics	No. of metastases (%)		P*
	Cohort 1	Validation cohort	
Total No. of metastases	338 (100)	103 (100)	
Location			1.00
Liver	331 (97.9)	103 (100)	
Lung	7 (2.1)	0 (0)	
Lesion size, mm			.75
Mean	21.82	20.77	
Range	(2–100)	(2–110)	
SD	18.76	20.68	
Metastasis surgery R status			.97
R0	303 (89.6)	98 (95)	
R1	17 (5)	5 (5)	
Preoperative treatment			<.0001
None	44 (13)	0 (0)	
Chemotherapy‡	46 (13.6)	44 (43)	
Chemotherapy + anti-VEGF§	130 (38.5)	44 (43)	
Chemotherapy + anti-EGFR‖	118 (34.9)	15 (15)	
Pathological response			
Tumor regression grade¶			<.0001
1	22 (6.5)	2 (2)	
2	69 (20.4)	18 (17.5)	
3	68 (20.1)	27 (26.2)	
4	102 (30.2)	51 (49.5)	
5	74 (21.9)	5 (4.8)	
Tumor regression grade¶			.91
1–2–3	159 (47)	47 (45.6)	
4–5	176 (52.1)	56 (54.4)	
Viable cells, %			.99
<50	158 (46.7)	45 (43.7)	
>50	176 (52.1)	58 (56.3)	
Fibrosis, %			.93
<50	227 (67.2)	80 (77.7)	
>50	100 (29.6)	23 (22.3)	

*The P values were assessed based on a multilevel model approach using a generalized linear mixed model fit for a binary response variable by a maximum likelihood (Laplace Approximation) method.

†Metastasis surgery R status refers to the surgical margin of tumor resection. R0 indicates that no tumor cells are seen microscopically. R1 indicates that tumor cells can be seen microscopically.

‡Chemo: oxaliplatin or irinotecan + fluoropyrimidine.

§Anti-VEGF: bevacizumab or cediranib.

‖Anti-EGFR: cetuximab or panitumumab.

¶Tumor regression grade in the least responding metastasis/patient.

Intrametastatic Immune Infiltrate and Immunoscore

Immune cells (CD3, CD8, CD45RO, CD20, and FOXP3) infiltrating the center (CT) and the invasive margin (IM) of metastases were quantified by immunohistochemistry on formalin-fixed paraffin-embedded tissues (see the Supplementary Methods, available online). Immune densities (cells/mm^2) were used to calculate the CD3/CD8 Immunoscore (I) and CD8/CD20 TB score (16). The Immunoscore ranges from 0 (I0), when low densities of

ARTICLE

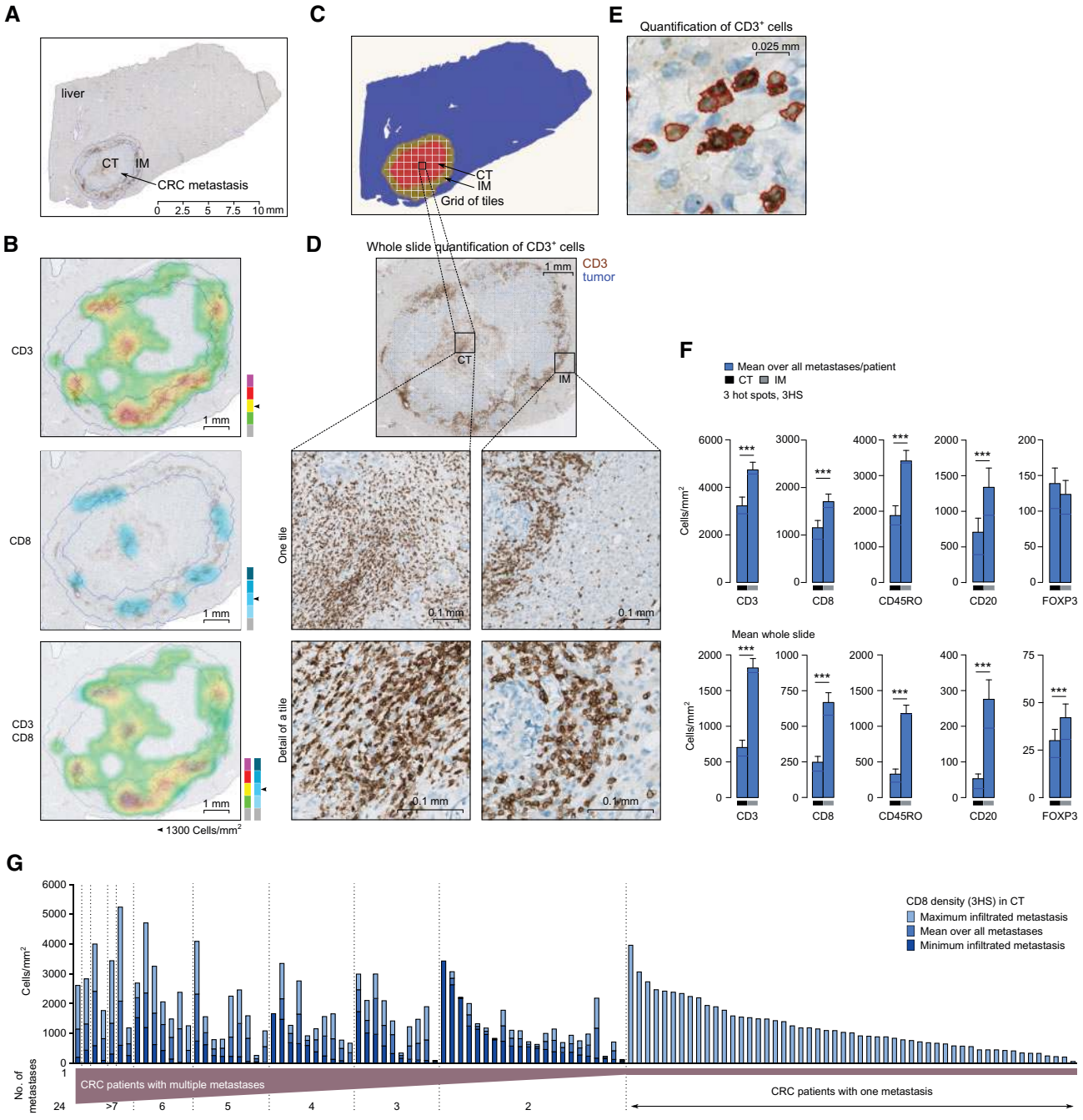

Figure 1. The immune microenvironment of distant metastases from colorectal cancer (CRC) patients. Curatively resected metastases (n = 338) from 114 CRC patients were quantified by immunohistochemistry on whole slide sections for immune infiltrates. **A)** The center (CT) and the invasive margin (IM) of each metastasis were defined, and most metastases were disseminated in the liver. **B)** Intrametastatic distribution of CD3 and CD8 infiltrate is shown by a low-to-high density color gradient from **gray to purple and dark azure**, respectively. The same density scale was applied for both CD3 and CD8 and for the combined heatmap. **C)** Immune markers were digitally quantified in a grid of tiles covering both metastatic regions. **D)** Representative whole slide immunohistochemistry of the CD3-positive cells for one tile in the CT and IM (CD3 in **brown**, tumor in **blue**). **Scale bars** represent 10, 1, 0.1, and 0.025 mm in (**A, B, D, and E**), respectively. **E)** Quantification of CD3-positive cells. **F)** Global (whole slide) and peak density (three hot spots [3HS]) for CD3, CD8, CD45RO, CD20, and FOXP3 in the CT (**black**) and IM (**gray**). The density was calculated as the number of positive cells/mm^2. For patients with multiple metastases, the average density over all metastases was calculated. A two-sided paired *t* test was applied to compare CT with IM (***$P < .001$). **Bar charts** represent the mean density per patient, and the **error bars** show 95% confidence intervals. **G)** CD8 density (3HS) quantified in the CT of the minimum (**dark blue**) and maximum (**light blue**) infiltrated metastasis of each patient. CD8 mean density over all metastases is shown in **blue**. Patients were sorted based on the number of metastases. CRC = colorectal cancer; CT = center; IM = invasive margin.

both markers are found in CT and IM, to 4 (I4), when high CD3 and CD8 densities are found in both regions. For patients with multiple metastases, the mean immune densities of all metastases, the least and the most-infiltrated metastases, and a randomly selected metastasis per patient were investigated.

Statistical Analysis

Kaplan-Meier curves were used to assess the impact of immune cell densities and Immunoscore on overall (OS) and disease-free survival (DFS). Univariate analysis of clinical and pathological

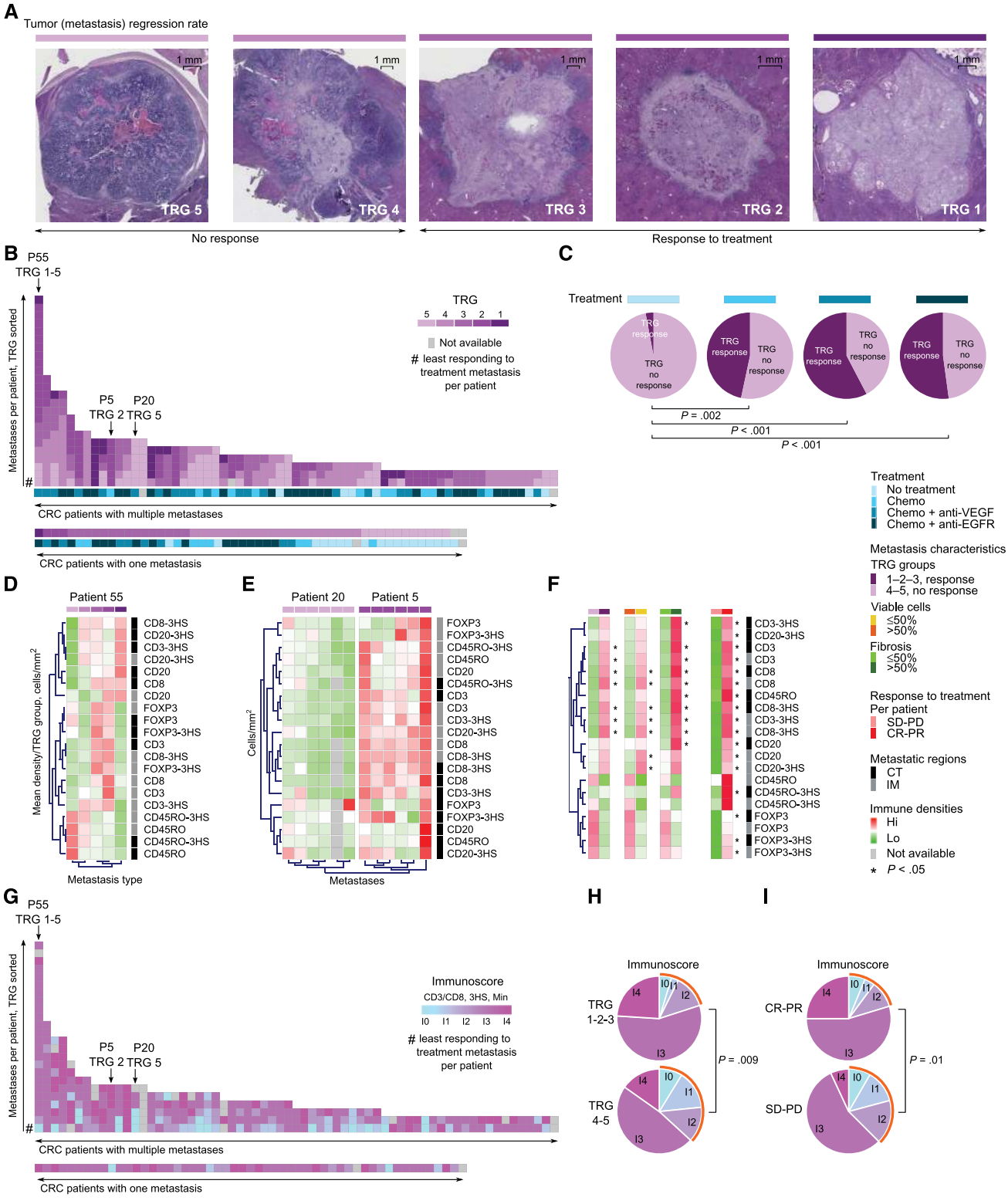

Figure 2. Metastasis immune infiltrate and response to preoperative treatment. **A)** Representative examples of tumor regression grade (TRG) categories according to the Rubbia-Brandt classification. **Scale bars** represent 1 mm. Response to treatment: TRG 1 (complete), 2 (major), and 3 (minor). Nonresponders: TRG 4 and 5. **B)** TRG was assessed in each metastasis (n = 338) of 114 preoperatively treated CRC patients. Patients with one or several metastases are shown. TRG is represented with a **purple gradient** scaling from **light** (no response) to **dark** (response) **purple**. Missing data are shown in **gray**. **B and G)** Multiple metastases of a patient are sorted based on the TRG, and the metastasis with the least response to treatment is marked with #. Patients with a heterogeneous (P55: TRG 1–5) or homogeneous (P5: TRG 2 and P20: TRG 5) response to treatment are highlighted. **C)** Proportion of responding (TRG 1–2–3) and nonresponding (TRG 4–5) patients in groups defined based on treatment. Nontreated patients, patients treated with chemotherapy (oxaliplatin or irinotecan and fluoropyrimidines), chemotherapy and anti-VEGF or anti-EGFR are shown with a **color gradient** scaling from **light to dark blue** (*P* values were assessed by multilevel analysis). **D–F)** Intrametastatic densities (cells/mm^2) of CD3, CD8, CD45RO, FOXP3,

parameters was performed using the log-rank test. The Cox proportional hazards model was performed to test the simultaneous influence on OS and DFS of all covariates. The assumption of the proportionality was assessed by the proportional hazards assumption (PHA) test. On the patient level, the *t* test and the Wilcoxon-Mann-Whitney test were applied, as well as the Fisher exact test for categorical values. To account for the dependency among the metastases from the same patient, all analyses on the metastasis level were done based on a multilevel model approach by using a generalized linear mixed model fit by maximum likelihood (Laplace Approximation) with a fixed predictor per individual level. All tests were two-sided, and a *P* value of less than .05 was considered statistically significant. Log-rank *P* values obtained for markers dichotomized using the minimal *P* value approach were corrected (20). Markers were evaluated using the Brier score (21). The likelihood ratio test was applied to compare two models. The predictive performance of the models was assessed by Harrell's concordance index (C-index) (22), and the time-dependent C-index (C_τ) was derived from time-dependent receiver operating characteristic curve (ROC) curve analysis (23). The Hosmer-Lemeshow test, adjusted for survival data using 10 subgroups, was applied to test the goodness of fit (24). Sensitivity was assessed by ROC curves. All analyses were performed using the R mlmRev, survival, Misc, and survMisc packages.

Results

The Immune Microenvironment of Distant Metastases From Patients With CRC

To enhance survival, complete surgical resection of all metastases was performed for 153 stage IV patients (Table 1; Supplementary Table 1, available online) (25,26). All 338 metastases (cohort 1) were investigated in relation to their immune infiltrates. Whole slides with metastasis sections were stained for major adaptive immune subsets (see the "Methods" section and the Supplementary Methods, available online). The IM and CT were marked on each of the stained slides (Figure 1A). Areas with dense infiltration of each immune subtype could be shown in both tumor regions (Figure 1B). The immune quantification was performed automatically using a grid of tiles fully covering the metastasis (Figure 1C), like that illustrated for CD3 (Figure 1D). All positive stained cells were detected and counted (Figure 1E). The global immune cell densities and the most-infiltrated tiles (three hot spots [3HS]) were statistically significantly higher in the IM than in the CT, except for FOXP3-3HS (Figure 1F). At the cohort level, CD3 density varied in the CT between 22 and 13 746 cells/mm^2 and was similar in patients with one or multiple metastases (Supplementary Figure 1A, available online). An intermetastatic immune variability among metastases of the same patient was also observed, like that illustrated for CD8 (Figure 1G). The patient with the highest CD8 variability had 5326 cells/mm^2 in the CT of the most-infiltrated metastasis, and just 685 cells/mm^2 in the CT of the least-infiltrated one (Figure 1G). On the other hand, a part of the cohort had a uniform infiltrate, with a minimum variation of approximately 30 CD8 cells/mm^2 per patient. CD3 infiltrate variation is illustrated in Supplementary Figure 1B (available online).

Relationship Between the Intrametastatic Immune Infiltrate and Response to Preoperative Treatment

Intrametastatic immune densities were investigated in relation to the response to preoperative treatment (TRG) (Figure 2A) for each of the 338 metastases. TRG varied between patients with one metastasis (Figure 2B). Patients with multiple metastases had different rates of response to treatment for each metastasis, such as P55 (all TRG grades). Some patients had a uniform response in all metastatic lesions, such as P5 (TRG 2) and P20 (TRG 5). As expected, treated patients more frequently had regressing tumors than untreated patients, but the multilevel analysis of responding (TRG 1–2–3) and nonresponding (TRG 4–5) patients (Figure 2C) showed no statistically significant difference between treatment-based groups.

Interestingly, immune densities, except for CD45RO, were higher in metastases that regressed compared with the not-responding metastases of the same patient (Figure 2D). The highest CD3 and CD8 infiltrate in the CT, as well as high CD20 densities in both CT and IM regions, were quantified in the metastasis with the best tumor regression rate (TRG 1). A statistically significantly higher amount of CD3, CD8, and CD45RO infiltrated the CTs and IMs of metastases from a responding patient, and statistically significantly more B cells (CD20) were found at their IMs compared with nonresponding metastases. No difference was observed for FOXP3 (Figure 2E; Supplementary Figure 1C, available online). At the cohort level, the immune adaptive cell densities were statistically significantly higher in TRG 1–2–3 metastases compared with TRG 4–5 metastases, except for CD45RO and FOXP3 in both tumor regions (Figure 2F; Supplementary Figure 1, D and E, available online). Overall, metastases showing a pathological response had statistically significantly higher CD3, CD8, and CD20 immune cell densities in both regions compared with metastases without histological response. Conversely, regulatory T cell densities were lower in responding metastases compared with those with absence of response. Similar results were also observed for radiological evaluation of metastases. Responding patients (CR-PR) had statistically significantly higher immune infiltrate than nonresponders for all immune types, with the exception of CD45RO in IM (Figure 2F).

Next, CD3 and CD8 densities were used to calculate the Immunoscore for each of the 338 metastases from cohort 1 (Figure 2G; Supplementary Figure 1C, available online). Using multilevel analysis of nested data for patients having at least

Figure 2. Continued
and CD20 were quantified on whole slide metastasis sections or as 3HS in the center (CT; **black**) and invasive margin (IM; **gray**). Data were normalized in Genesis and hierarchically clustered. Immune densities were scaled from low (**green**) to high (**red**) in patients with heterogeneous **(D)** or homogeneous **(E)** TRG rate of their metastases. **F)** The mean immune densities were shown in metastatic groups defined based on the percentage of viable cells (≤50%, >50%), fibrosis (≤50%, >50%), response rate (TRG 1–2–3, TRG 4–5), or in groups of patients who respond (CR-PR) or do not respond (SP-PD) to the treatment. All *P* values of less than .05 were marked with *. **G–I)** Immunoscore was calculated based on CD3 and CD8 T lymphocyte densities from the CT and IM of each resected metastasis. The Immunoscore was scaled from **azure** (I0, both markers low in CT and IM) to **dark pink** (I4, both markers high in CT and IM). The distribution of Immunoscore 0–1–2 vs 3–4 in metastasis groups defined was based on TRG (responding TRG 1–2–3, nonresponding TRG 4–5; multilevel analysis, $P = .009$) **(H)**, and on responding (CR-PR) and nonresponding patients (Fisher exact test, $P < .01$) **(I)**. All statistical tests were two-sided. CRC = colorectal cancer grade; CR-PR = complete and partial response; CT = center; IM = invasive margin; SD-PD = stable and progressive disease; TRG = tumor regression grade.

Table 2. Univariate analysis of disease-free survival and overall survival among preoperatively treated patients with UICC-TNM stage IV colorectal cancer according to immune parameters*

	Disease-free survival					Overall survival				
Immune parameters	No. of patients (%)	Rate at 5 y (95% CI), %	HR‡ (95% CI)	P‡,§	Predictive Accuracy (%) C-index	No. of patients (%)	Rate at 5 y (95% CI), %	HR (95% CI)	P‡	Predictive accuracy C-index, %
CD3 CT					59.4					61.5
Lo	28 (31.1)	15.1 (5.8 to 38.9)	1.0 (reference)			27 (30.7)	32.5 (15.2 to 69.3)	1.0 (reference)		
Hi	62 (68.9)	23.3 (12.6 to 43.1)	0.6 (0.41 to 0.89)	.32		61 (69.3)	58.8 (42.8 to 80.8)	0.41 (0.20 to 0.82)	.009	
CD3 IM					56.5					56.8
Lo	75 (83.3)	21.4 (13.1 to 34.8)	1.0 (reference)			73 (83)	51.2 (37.2 to 70.5)	1.0 (reference)		
Hi	15 (16.7)	27.5 (9.8 to 77.0)	0.58 (0.33 to 1.02)	.93		15 (17)	46.2 (18.6 to 100.0)	0.53 (0.19 to 1.51)	.23	
CD3 CTIM					62.5					64.2
LoLo	28 (31.1)	15.1 (5.8 to 38.9)	1.0 (reference)			27 (30.7)	32.5 (15.2 to 69.3)	1.0 (reference)		
Het	47 (52.2)	25.7 (14.8 to 44.4)	0.71 (0.5 to 1.01)	.94		46 (52.3)	64.6 (48.3 to 86.3)	0.44 (0.21 to 0.93)	.03	
HiHi	15 (16.7)	27.5 (9.8 to 77.0)	0.43 (0.22 to 0.83)	.30		15 (17)	46.2 (18.6 to 100.0)	0.33 (0.11 to 1.01)	.04	
CD8 CT					62.6					65.8
Lo	29 (32.2)	7.9 (2.1 to 29.3)	1.0 (reference)			28 (31.8)	27.9 (13.6 to 57.6)	1.0 (reference)		
Hi	61 (67.8)	26 (14.3 to 47.3)	0.41 (0.26 to 0.64)	.004		60 (68.2)	62.5 (45.2 to 86.5)	0.31 (0.15 to 0.63)	<.001	
CD8 IM					58.7					61.3
Lo	19 (21.1)	5.3 (0.8 to 35.5)	1.0 (reference)			17 (19.3)	29.4 (12.7 to 68.0)	1.0 (reference)		
Hi	71 (78.9)	23.8 (13.1 to 43.2)	0.45 (0.28 to 0.71)	.027		71 (80.7)	56.9 (41.4 to 78.2)	0.42 (0.20 to 0.88)	.02	
CD8 CTIM					64.7					68.3
LoLo	15 (16.7)	6.7 (1.0 to 44.3)	1.0 (reference)			14 (15.9)	30.0 (12.4 to 72.8)	1.0 (reference)		
Het	18 (20)	7.4 (1.2 to 45.7)	1.0 (0.49 to 2.06)	1.00		17 (19.3)	26.6 (9.6 to 74.0)	1.01 (0.41 to 2.49)	.98	
HiHi	57 (63.3)	27.9 (15.4 to 50.5)	0.42 (0.25 to 0.69)	.02		57 (64.8)	64.9 (47.1 to 89.4)	0.3 (0.12 to 0.72)	.004	
CD20 CT					58.8					63.6
Lo	26 (29.2)	0.0 (0.0 to 0.0)	1.0 (reference)			25 (28.7)	27.4 (12.7 to 59.1)	1.0 (reference)		
Hi	63 (70.8)	28.3 (16.9 to 47.4)	0.45 (0.28 to 0.72)	.03		62 (71.3)	65.1 (50.7 to 83.6)	0.32 (0.16 to 0.64)	<.001	
CD20 IM					53.6					57.6
Lo	17 (19.1)	15.7 (4.9 to 50.7)	1.0 (reference)			16 (18.4)	21.1 (6.7 to 66.2)	1.0 (reference)		
Hi	72 (80.9)	21.6 (11.7 to 39.8)	0.91 (0.78 to 1.06)	1.00		71 (81.6)	60.6 (45.9 to 80)	0.39 (0.18 to 0.82)	.01	
CD20 CTIM					59.5					65.9
LoLo	7 (7.9)	0.0 (0.0 to 0.0)	1.0 (reference)			6 (6.9)	0 (NA to NA)	1.0 (reference)		
Het	29 (32.6)	11.2 (3.3 to 38.5)	0.7 (0.43 to 1.14)	1.00		29 (33.3)	38.4 (21.4 to 69)	0.33 (0.12 to 0.88)	.02	
HiHi	53 (59.6)	28.3 (15.7 to 50.9)	0.37 (0.19 to 0.72)	.08		52 (59.8)	73.7 (60.2 to 90.4)	0.14 (0.05 to 0.38)	<.001	
Immunoscore (I 0–1–2 = 0, I 3–4 = 1)										65.9
I 0–1–2	40 (44.4)	12.3 (4.9 to 30.6)	1.0 (reference)		63.1	38 (43.2)	32.5 (17.2 to 61.4)	1.0 (reference)		
I 3-4	50 (55.6)	27.9 (15.2 to 51.3)	0.45 (0.28 to 0.7)	.02		50 (56.8)	64.6 (46.6 to 89.6)	0.32 (0.15 to 0.66)	.001	
TB score (TB 0–1–2 = 0, TB 3–4 = 1)					63.1					67.8
TB 0–1–2	25 (28.1)	5.0 (0.8 to 32.4)	1.0 (reference)			24 (27.6)	21.4 (9.2 to 49.8)	1.0 (reference)		
TB 3–4	64 (71.9)	25.7 (14.2 to 46.6)	0.36 (0.22 to 0.57)	<.001		63 (72.4)	63.7 (46.4 to 87.5)	0.25 (0.12 to 0.51)	<.001	

*Immune densities measured as three hot spots in the least-infiltrated metastasis/patient. C-index: Harrell's concordance index corresponds to the area under the receiver operating characteristic curve; CI = confidence interval; CT = center of the tumor (metastasis); CTIM = both tumor regions; Het = Hi/Lo and Lo/Hi; Hi = high cell density (optimal cutoff); HR = hazard ratio; IM = invasive margin; Immunoscore = marker combination CD3-CTIM CD8-CTIM; Lo = low cell density (optimal cutoff); TB score = marker combination CD8-CTIM CD20-CTIM.
†Heuristic shrinkage factor. Corrected by Holländer et al.
‡Two-sided log-rank P value.
§P value correction with Altman et al.

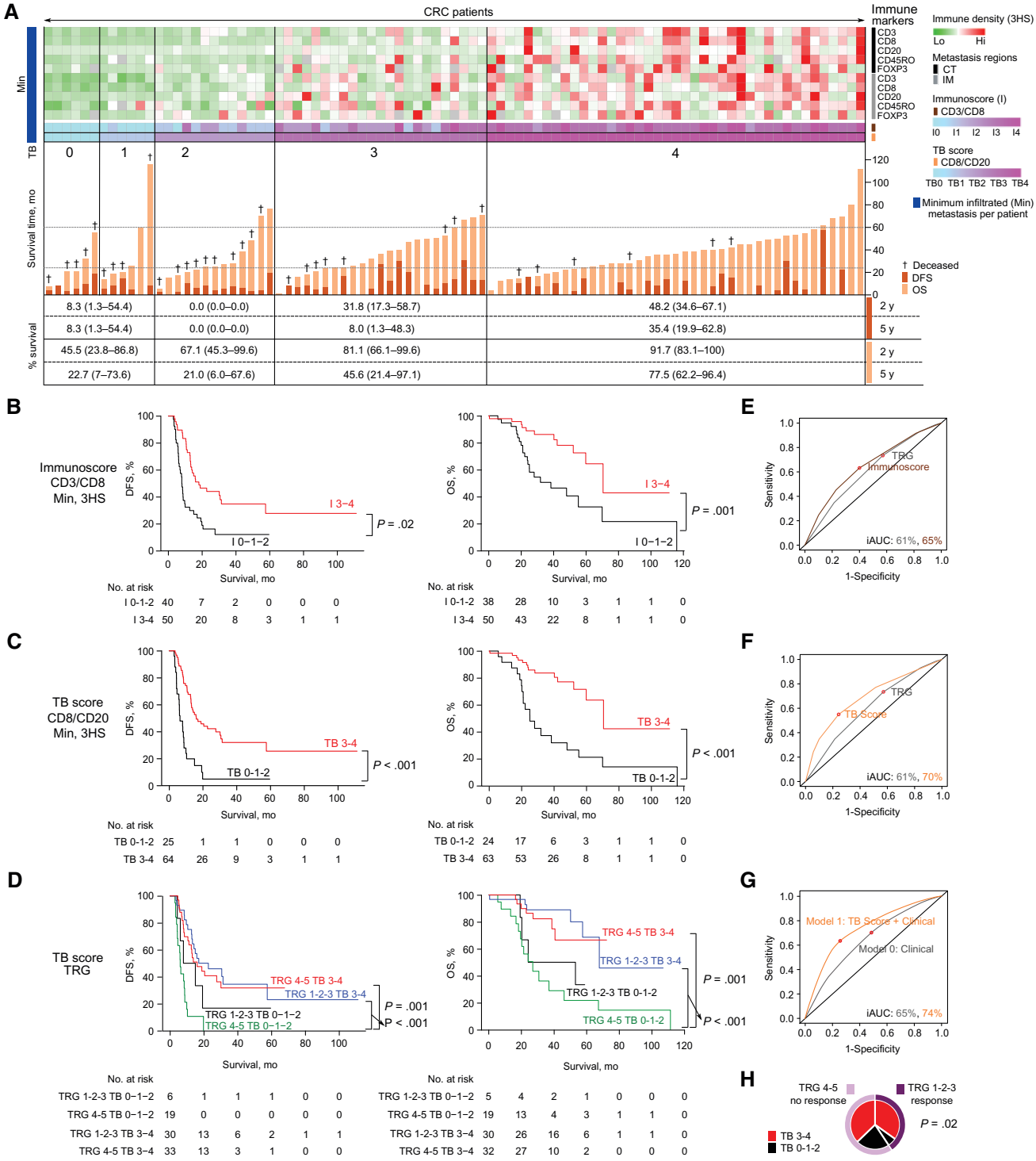

Figure 3. Intrametastatic immune infiltrate and survival of patients. CD3, CD8, CD45RO, CD20, and FOXP3 densities were quantified (3HS) in the lowest (min; **dark blue**)-infiltrated metastases in two tumor regions: center (CT; **black**) and the invasive margin (IM; **gray**). **A)** Immune densities (3HS) in the lowest (**dark blue**)-infiltrated metastases. The data were normalized by mean subtraction and division by standard deviation. Low and high immune densities are shown in **green** and **red**, respectively. Missing values are shown in **light gray**. Immunoscore (I) and TB score were determined based on the minimum infiltrated metastases. Five groups of patients were defined based on the density of CD8 and CD20 in the CT and IM of the metastasis (minimum *P* value cutoff): TB 0 (0Hi), TB 1 (1Hi), TB 2 (2Hi), TB 3 (3Hi), TB 4 (4Hi). Immunoscore groups are defined similarly. Patients are sorted based on the TB score. Survival time (months) is shown for each patient. Disease-free survival (DFS) and overall survival (OS) are shown in **dark and light orange**. Deceased patients are marked with a †. Follow-up at two and five years is shown with **dashed lines**. The percentage of TB 0–1, TB 2, TB 3, and TB 4 disease-free and living patients after two and five years of follow-up is also shown. Kaplan-Meier estimates and log-rank test DFS and OS according to the Immunoscore **(B)**, TB score **(C)**, and tumor regression grade (TRG) and TB score combined **(D)**. The number of patients at risk for each group is shown. **B)** Patients with Immunoscore 0, 1, and 2 (I 0–1–2, **black**) are grouped. Similarly, patients with I 3 and I 4 are grouped (I 3–4, **red**). **C)** Patients with TB 0–1–2 and TB 3–4 are shown in **black and red**, respectively. **D)** Patients with TRG 1–2–3 and TB 3–4 or TB 0–1–2 are shown in **blue and black**, respectively. Patients with TRG 4–5 and TB 3–4 or TB 0–1–2 are shown in **red and green**, respectively. Receiver operating characteristic (ROC) curves for OS representing the TRG, Immunoscore **(E)**, and TB

three metastases, the one that responded the least to treatment had statistically significantly lower infiltration than the other metastatic lesions ($P = .04$). Inversely, high-Immunoscore metastases had statistically significantly better pathological responses (TRG 1–2–3) (Figure 2H) on the metastasis level and radiological (CR-PR) responses (Figure 2I) on the patient level. However, many of the TRG 4–5 classified metastases were strongly infiltrated with immune cells (Figure 2H).

Metastasis Immune-Based Scores and Patient Survival

The survival of the patients was further investigated in relation to clinical and histopathological parameters. Among these, only the metastatic load represented by the number of metastases impacted both the DFS and OS (Supplementary Tables 2 and 3 and Supplementary Figure 2, A and B, available online).

Further, because immune cells were nonuniformly distributed between metastases of the same patient, their impact on survival was assessed based on CT and IM densities from the minimum infiltrated metastasis. High immune densities, high Immunoscore, and high TB score were statistically significantly associated with prolonged patient survival and decreased relapse incidence (Table 2; Supplementary Table 4, available online). In addition, a high variability of CD8 and CD20 infiltrates among metastases of the same patient statistically significantly increased the risk to relapse and death (Supplementary Table 5, available online).

The immune landscape of the least-infiltrated metastases was next visualized by density heatmap (Figure 3A) in combination with the survival time of each patient. TB 4 patients had a statistically significantly prolonged DFS and OS compared with patients with low infiltrate. At five years of follow-up, 77.5% of the TB 4 patients were alive and 64.6% of these patients were not relapsing. In comparison, 91.7% of the TB 0–1 patients had recurrence and only 22.7% of them were alive (Supplementary Figure 2, C and D, available online). Patients with a high Immunoscore in their least-infiltrated metastasis had a statistically significantly lower risk of relapse (I 3–4: DFS rate = 27.9%, 95% CI = 15.2 to 51.3; vs I 0–1–2: DFS rate = 12.3%, 95% CI = 4.9 to 30.6; HR = 0.45, 95% CI = 0.28 to 0.70, $P = .02$) and a prolonged survival (I 3–4: OS rate = 64.6%, 95% CI = 46.6 to 89.6; vs I 0–1–2: OS rate = 32.5%, 95% CI = 17.2 to 61.4; HR = 0.32, 95% CI = 0.15 to 0.66, $P = .001$, C-index = 65.9%) compared with patients with a low Immunoscore (Figure 3B and Table 2; Supplementary Figure 2, C and D, and Supplementary Table 4, available online). Similar results were obtained for the TB score (TB 3–4: DFS rate = 25.7%, 95% CI = 14.2 to 46.6; vs TB 0–1–2: DFS rate = 5.0%, 95% CI = 0.8 to 32.4; HR = 0.36, 95% CI = 0.22 to 0.57, $P < .001$; TB 3–4: OS rate = 63.7%, 95% CI = 46.4 to 87.5; vs TB 0–1–2: OS rate = 21.4%, 95% CI = 9.2 to 49.8; HR = 0.25, 95% CI = 0.12 to 0.51, $P < .001$, C-index = 67.8%). High–TB score and -Immunoscore patients had a median survival of 70.5 months, while low-score patients survived only 25.1 to 38.3 months. The accuracy of Immunoscore and TB score in identifying patients with high risk of death was also demonstrated in a validation cohort (Table 1; Supplementary Figure 3, A and B, and Supplementary Table 1, available online). Additionally, to illustrate the reliability of the immune infiltrate in predicting survival, a second method for the classification of the patients was applied. Cohort percentiles with different immune density levels for Immunoscore and TB score markers were considered. A good discrimination between the top 25.0% highest-infiltrated patients and the lowest-infiltrated (0.0%–25.0%) or intermediate (25.0%–75.0%) groups was shown at DFS for Immunoscore (C-index = 59.9) and TB score (C-index = 56.8) (Supplementary Figure 3C, available online). Similar results were observed in the validation cohort (Supplementary Figure 3D, available online). These highly infiltrated patients had also statistically significantly prolonged overall survival, as illustrated for Immunoscore (C-index = 65.6 and 60.6) and TB score (C-index = 63.7 and 56.8) in both cohorts (Supplementary Figure 3, E and F, available online). The immunoscore defined based on both, the minimum P value approach, or the percentile method accurately identified patients at risk of relapse and death (Figure 3D; Supplementary Figure 3, G and H, available online).

A statistically significant prolonged disease-free survival (HR = 0.50, 95% CI = 0.29 – 0.87, $P = .01$) was observed for patients treated with chemotherapy and anti-EGFR compared with patients treated with chemotherapy and anti-VEGF (Supplementary Figure 4A, available online). When investigating the DFS within each treatment group (chemotherapy and anti-EGFR or anti-VEGF) in relation to the Immunoscore, both groups showed a statistically significantly lower risk of relapse in patients with a high Immunoscore compared with patients with a low Immunoscore (HR = 0.47, 95% CI = 0.22 to 1.01, $P = .05$; and HR = 0.20, 95% CI = 0.08 to 0.47, $P < .001$, respectively) (Supplementary Figure 4, B and C, available online). There was no difference in the survival of the patients based on their tumor regression grade (Supplementary Figure 4D, available online). Instead, patients with a strong T and B cell infiltrate, even if classified as nonresponders, had a statistically significantly prolonged survival (HR = 0.25, 95% CI = 0.10 to 0.62, $P = .001$) compared with patients with low infiltrate (Figure 3D). ROC curve analysis revealed the better predictive performance of the Immunoscore and TB score compared with clinical parameters like TRG (Figure 3, E–G). Multilevel analysis of high- vs low-infiltrated patients was statistically significantly different ($P = .02$) in TRG-defined groups. A strong immune infiltrate was observed in the majority of the responders, and only 16.7% of these patients had low immune infiltrate (Figure 3H). On the other hand, 62.7% of the nonresponders had highly infiltrated metastases. Interestingly, such patients had a prolonged DFS (HR = 0.28, 95% CI = 0.15 to 0.52, $P = .001$) and OS (HR = 0.25, 95% CI = 0.10 to 0.62, $P = .001$), similar to patients that responded to treatment (Figure 3, D and H; Supplementary Figure 4E, available online). The immune infiltrate level was not influenced by the administrated chemotherapy regimen (Supplementary Figure 4F, available online).

Cox multivariable regression analysis of relevant clinical and immune parameters revealed that the TB score, node stage, preoperative treatment type, metastasis resection (R) status,

Figure 3. Continued

score **(F)** as well as the clinical model without (model 0) and with TB score (model 1). **G)** Integrated area under the ROC curve (iAUC). Points on the curves for the best separation of two groups are indicated in **red**. **G)** Clinical model 0 included the age, N stage, preoperative treatment type, metastasis surgery R status, two-stage hepatectomy, RAS mutation status, and TRG. **H)** Frequency of TB 3–4 (**red**) or TB 0–1–2 (**black**) patients in the TRG 1–2–3 (**dark purple**) and TRG 4–5 (**light purple**) groups. Multilevel analysis using a generalized linear mixed model fit by maximum likelihood (Laplace Approximation) was applied. All statistical tests were two-sided. CRC = colorectal; DFS = disease-free survival; OS = overall survival; TRG = tumor regression grade.

Table 3. Multivariable proportional hazard Cox analysis for OS and the minimal infiltrated metastasis stage IV colorectal cancer among patients with UICC-TNM

Model parameters	HR (95% CI)	P*	PHA test†	No. of patients	C-index (95% CI)	AIC
Model with relevant clinical parameters for OS before stepwise (stepAIC) selection				71	83.8 (76.8 to 90.9)	170.59
Age (<50 = 0, 50–60 = 1, 60–70 = 2, >70 = 3), y	1.57 (0.91 to 2.73)	.11	.93			
Tumor stage (T0–1–2 = 0, T3 = 1, T4 = 2)	1.37 (0.48 to 3.87)	.56	.69			
Node stage (N0 = 0, N + = 1)	3.63 (0.85 to 15.54)	.08	.04			
Tumor location (rectum = 0, sigmoid left colon = 1, right transverse colon = 2)	1.03 (0.42 to 2.51)	.95	.004			
Preoperative treatment type (chemo = 0, chemo + anti-VEGF = 1, chemo + anti-EGFR = 2)	2.43 (0.88 to 6.74)	.09	.58			
Histological grade/differentiation (well = 0, moderately = 1, poorly = 2)	0.84 (0.26 to 2.78)	.78	.38			
Metastasis surgery R status (R0 = 0, R1 = 1)‡	5.98 (0.99 to 36.07)	.05	.66			
Number of metastases per patient (<3 = 0, >3 = 1)	1.50 (0.37 to 6.13)	.58	.24			
Synchronous, metachronous metastasis (synchronous = 0, metachronous = 1)	1.14 (0.22 to 5.86)	.87	.22			
TRG (TRG 1–2–3 = 0, TRG 4–5 = 1)	2.64 (0.66 to 10.58)	.17	.97			
Two-stage hepatectomy (no = 0, yes = 1)	0.13 (0.01 to 1.27)	.08	.33			
Postoperative treatment (no = 0, yes = 1)	1.14 (0.40 to 3.27)	.81	.04			
Preoperative chemo type (FOLFOX = 0, FOLFIRI = 1, others = 2)	1.68 (0.74 to 3.84)	.22	.04			
RAS status (WT = 0, mutated = 1)	4.48 (1.22 to 16.48)	.02	.74			
TB (CD8/CD20) score (TB 0–1–2 = 0, TB 3–4 = 1)	0.14 (0.03 to 0.72)	.02	.86			
Model 0: final model for OS after stepwise (stepAIC) selection without marker				86	64.9 (54.3 to 75.6)	239.97
Age (<50 = 0, 50–60 = 1, 60–70 = 2, >70 = 3), y	1.05 (0.72 to 1.53)	.79	.89			
Node stage (N0 = 0, N + = 1)	1.63 (0.65 to 4.14)	.30	.10			
Preoperative treatment type (chemo = 0, chemo + anti-VEGF = 1, chemo + anti-EGFR = 2)	0.97 (0.59 to 1.61)	.92	.8			
Metastasis surgery R status (R0 = 0, R1 = 1)‡	1.67 (0.43 to 6.51)	.46	.62			
TRG (TRG 1–2–3 = 0, TRG 4–5 = 1)	2.00 (0.87 to 4.60)	.10	.27			
Two-stage hepatectomy (no = 0, yes = 1)	0.38 (0.08 to 1.82)	.23	.65			
RAS status (WT = 0, mutated = 1)	1.62 (0.71 to 3.70)	.26	.72			
Model 1: final model for OS after stepwise (stepAIC) selection with marker TB score				86	76.1 (66.1 to 86.0)	227.94
Age (<50 = 0, 50–60 = 1, 60–70 = 2, >70 = 3), y	1.11 (0.75 to 1.64)	.60	.83			
Node stage (N0 = 0, N + = 1)	1.43 (0.54 to 3.81)	.47	.14			
Preoperative treatment type (chemo = 0, chemo + anti-VEGF = 1, chemo + anti-EGFR = 2)	1.19 (0.66 to 2.16)	.56	.86			
Metastasis surgery R status (R0 = 0, R1 = 1)‡	2.72 (0.69 to 10.77)	.15	.44			
TRG (TRG 1–2–3 = 0, TRG 4–5 = 1)	1.31 (0.56 to 3.11)	.53	.33			
Two-stage hepatectomy (no = 0, yes = 1)	0.27 (0.06 to 1.27)	.10	.85			
RAS status (WT = 0, mutated = 1)	1.44 (0.59 to 3.53)	.43	.97			
TB (CD8/CD20) score (TB 0–1–2 = 0, TB 3–4 = 1)	0.20 (0.08 to 0.48)	<.001	.32			
Likelihood ratio test: model 1 vs model 0		<.001§				

(continued)

Table 3. (continued)

Model parameters	HR (95% CI)	P*	PHA test†	No. of patients	C-index (95% CI)	AIC
Model 2: final model for OS after stepwise (stepAIC) selection with marker immunoscore				86	75.3 (65.4 to 85.1)	230.90
Age (<50 = 0, 50–60 = 1, 60–70 = 2, >70 = 3), y	1.19 (0.80 to 1.78)	.39	.62			
Node stage (N0 = 0, N+ = 1)	1.22 (0.45 to 3.26)	.70	.09			
Preoperative treatment type (chemo = 0, chemo + anti-VEGF = 1, chemo + anti-EGFR = 2)	1.11 (0.63 to 1.96)	.71	.78			
Metastasis surgery R status (R0 = 0, R1 = 1)‡	1.33 (0.33 to 5.37)	.69	.68			
TRG (TRG 1–2–3 = 0, TRG 4–5 = 1)	1.48 (0.63 to 3.50)	.37	.26			
Two-stage hepatectomy (no = 0, yes = 1)	0.23 (0.05 to 1.08)	.06	.67			
RAS status (WT = 0, mutated = 1)	1.27 (0.53 to 3.01)	.59	.97			
Immunoscore (I 0–1–2 = 0, I 3–4 = 1)	0.24 (0.10 to 0.58)	.001	.23			
Likelihood ratio test: model 2 vs model 0		<.001§				

*The P values were assessed by a Wald test within a multivariable Cox proportional hazards model. All P values are two-sided. AIC = Akaike Information Criterion; anti-EGFR: cetuximab or panitumumab; anti-VEGF: bevacizumab or cediranib; C-index: Harrell's concordance index corresponds to the area under the receiver operating characteristic curve; chemo: FOLFOX, FOLFIRI, or others; FOLFIRI = fluoropyrimidine + irinotecan and others: fluoropyrimidine alone or fluoropyrimidine + oxaliplatin + irinotecan; FOLFOX: fluoropyrimidine + oxaliplatin; HR = hazard ratio; Immunoscore: CD3CT/IM-CD8CT/IM based on the minimum infiltrated metastasis, minimum P value DFS cutoff with four groups: (I4)-4Hi, (I3)-3Hi, (I2)-2Hi, (I1)-1Hi), (I0)-0Hi); N = node; T = tumor; TRG = tumor regression grade in the least-responding metastasis/patient TB (CD8/CD20) score: CD8CT/IM-CD20CT/IM based on the minimum infiltrated metastasis, minimum P value DFS cutoff with four groups: (TB4)-4Hi, (TB3)-3Hi, (TB2)-2Hi, (TB1)-1Hi), (TB0)-0Hi); WT = wild type.
†PHA test P < .05 violates the hazards assumption; parameter has to be excluded.
‡Metastasis surgery R status refers to the surgical margin of tumor resection. R0 indicates that no tumor cells are seen microscopically; R1 indicates that tumor cells can be seen microscopically.
§P value was calculated using a two-sided likelihood ratio test.

TRG status, and RAS status remained statistically significantly associated with OS (Table 3). Interestingly, out of these markers, only the TB score remained statistically significant (HR = 0.20, 95% CI = 0.08 to 0.48, P < .001) in the final model 1 after Akaike Information Criterion (AIC) stepwise selection (Table 3). The predictive accuracy of the model 1 including TB score (C-index = 76.1, 95% CI = 66.1 to 86.0) was statistically significantly increased (likelihood ratio test P < .001) compared with model 0 including only clinical parameters (C-index = 64.9, 95% CI = 54.3 to 75.6) (Figure 3G). The Immunoscore also had a similar impact (HR = 0.24, 95% CI = 0.10 to 0.58, P = .001; C-index = 75.3, 95% CI = 65.4 to 85.1) when added in the final model (Table 3). The TB score was also statistically significantly associated with DFS, as was the number of metastases per patient (Supplementary Table 6, available online), parameters that remained statistically significant in the model after the AIC stepwise selection. Markers included in the OS final model were also tested for DFS, and similar results were obtained (Supplementary Table 6, available online). Similar results for OS and DFS were also obtained considering the RECIST evaluation (Supplementary Table 7, available online) or untreated patients (Supplementary Table 8, available online) in the model. Thus, the immune parameters remained statistically significant in multivariable analysis for DFS and OS, whereas histopathological parameters, including TRG, did not.

Discussion

We performed comprehensive analyses of the intrametastatic immune infiltrates in 153 stage IV CRC patients undergoing complete curative metastatic resection. All metastases of a patient were investigated, thus extending previous knowledge (27–30). Whole slide automatic quantification assembled detailed information about the spatial immune cell distribution within metastases.

Like primary tumors (31), metastases were infiltrated with adaptive immune cells in a nonuniform manner, and densely infiltrated areas could be observed in both tumor regions. Metastases of the same patient were infiltrated with diverse amounts of immune cells, each responding differently to treatment. Interestingly, there was a statistically significantly higher frequency of Immunoscore 3–4 metastases in patients achieving pathological and radiological responses. This heterogeneity of the tumor microenvironment (32), in addition to the genetic heterogeneity of metastatic disease (33,34), seems to relate to treatment response.

Out of all metastases of a patient, the least-infiltrated metastasis had a particular importance; it was statistically significantly associated with prolonged survival. Immunoscore and TB score evaluated as the mean of all metastases or on a random selected metastasis were less informative but still statistically significant, in contrast to the most-infiltrated metastasis. Recently, a genetic metastatic heterogeneity was described (35,36).

T cells of a randomly selected metastasis have previously been associated with increased survival (27–30). The least-infiltrated metastasis is likely least affected by immune-based elimination and could further promote metastatic progression (37). Even if logistically difficult, this highlights the importance of evaluating immune parameters from multiple metastases and metastasis heterogeneity in immunotherapy clinical trials. Immunoscore remained the only statistically significant parameter for DFS and OS during multivariable analysis involving

relevant clinico-pathological factors after metastasis resection (3,4,7). Cox multivariable analysis supports the advantage of Immunoscore and TB score compared with histopathologic features, including TRG, in predicting patients' survival.

The histological response of metastases to preoperative treatment (38) has been described as a prognostic factor (7,39). The quality and heterogeneity of histological data could affect the prognostic and predictive significance of the TRG, as shown in rectal cancer (40). We report here that the immune infiltrate and Immunoscore of metastases are associated with the rate of the response to treatment and with the survival of the patients. A strong infiltrate with adaptive immune cells was prolonging the survival of the patients, even if they were classified as non-responders. These findings underline the importance of immunological markers in determining the prognosis and response to therapy. The accuracy, reproducibility, and prognostic value of the Immunoscore were validated by an international consortium (41).

Limitations of the study might be due to the administration of heterogeneous treatments. However, in our cohorts, preoperative treatments were all systemically administrated, and no difference in the immune infiltrate level between oxaliplatin- and irinotecan-treated patients was observed. The impact of local administration of treatment via intrahepatic infusion should be assessed in future studies.

Our results suggest that within metastatic CRC the adaptive immune response may play a role in preventing tumor recurrence. Evidence for immunoediting (42,43) and the role of cytokines were also previously highlighted as mechanisms of increased intratumoral T cell densities (31,42,44–49). The natural immunity and long-lasting capacity of memory T cells (50) could play a central role in patients' survival. Our data suggest that DFS and OS in stage IV patients are largely governed by the state of the local adaptive immune response within the metastases, in particular the least-infiltrated metastasis. This provides further support for immunotherapy, aiming at modulating the preexisting immunity, as a cornerstone of cancer treatment.

Funding

This work was supported by grants from the National Cancer Institute of France (INCa), the Canceropole Ile de France, MedImmune, INSERM, Cancer Research for Personalized Medicine (CARPEM), the Paris Alliance of Cancer Research Institutes (PACRI), the LabEx Immuno-oncology, the Transcan ERAnet European Project, the Association pour la Recherche contre le Cancer (ARC), the Advanced Bioinformatics Platform for Personalised Cancer Immunotherapy (APERIM), H2020 (PHC-32 grant No. 633592), the Fondation St-Luc, and the Cliniques des Pathologies Tumorales du Colon et du Rectum (CPTCR) of the Cliniques Universitaires St-Luc.

Notes

Authors: Bernhard Mlecnik*, Marc Van den Eynde*, Gabriela Bindea*, Sarah E. Church, Angela Vasaturo, Tessa Fredriksen, Lucie Lafontaine, Nacilla Haicheur, Florence Marliot, Daphné Debetancourt, Géraldine Pairet, Anne Jouret-Mourin, Jean-Francois Gigot, Catherine Hubert, Etienne Danse, Cristina Dragean, Javier Carrasco, Yves Humblet, Viia Valge-Archer, Anne Berger, Franck Pagès, Jean-Pascal Machiels, Jérôme Galon

*Authors contributed equally to this work.

Affiliations of authors: Laboratory of Integrative Cancer Immunology, INSERM, UMRS1138, Paris, France (BM, MVdE, GB, SEC, AV, TF, LL, FM, AB, FP, JG); Université Paris Descartes, Sorbonne Paris Cité, UMRS1138, Paris, France (BM, MVdE, GB, SEC, AV, TF, LL, FM, AB, FP, JG); Sorbonne Universités, UPMC Univ Paris 06, UMRS1138, Centre de Recherche des Cordeliers, Paris, France (BM, MVdE, GB, SEC, AV, TF, LL, FM, AB, FP, JG); Inovarion, Paris, France (BM); Department of Medical Oncology, Cliniques Universitaires St-Luc and Institut de Recherche Clinique et Experimentale (Pole MIRO), Institut Roi Albert II, Université Catholique de Louvain, Brussels, Belgium (MVdE, DD, GP, AJM, JFG, CH, ED, CD, YH, JPM); Department of Immunology, HEGP, Assistance Publique-Hopitaux de Paris, Paris, France (NH, FM, FP); AstraZeneca, Cambridge, UK (VVA); Departments of General and Digestive Surgery, HEGP, AP-HP, Assistance Publique-Hopitaux de Paris, Paris, France (AB); Grand Hopital de Charleroi, Charleroi, Belgium (JC).

The funders had no role in the design of the study; the collection, analysis, or interpretation of the data; the writing of the manuscript; or the decision to submit the manuscript for publication.

Author contributions: study concept and design: JG, MVdE, BM, GB; acquisition of data: MVdE, SEC, AV, TF, LF, NH, FM; analysis and interpretation of data: BM, MVdE, GB; drafting of the manuscript: JG, BM, MVdE, GB; critical revision of the manuscript: JG, BM, MVdE, GB, FP, JPM, VVA; statistical analysis: BM, GB; technical support: SEC, AV, TF, LF, NH, FM; material support: MVdE, DD, GP, AJM, JFG, CH, ED, CD, JC, YH, AB, FP; study supervision: JG.

Disclosures: patents: JG, FP, BM, GB; cofounder of HalioDx company: JG.

References

1. Adam R, Wicherts DA, de Haas RJ, et al. Patients with initially unresectable colorectal liver metastases: Is there a possibility of cure? *J Clin Oncol*. 2009; 27(11):1829–1835.
2. Ruers T, Punt C, Van Coevorden F, et al. Radiofrequency ablation combined with systemic treatment versus systemic treatment alone in patients with non-resectable colorectal liver metastases: A randomized EORTC Intergroup phase II study (EORTC 40004). *Ann Oncol*. 2012;23(10):2619–2626.
3. Vigano L, Capussotti L, Lapointe R, et al. Early recurrence after liver resection for colorectal metastases: Risk factors, prognosis, and treatment. A LiverMetSurvey-based study of 6,025 patients. *Ann Surg Oncol*. 2014;21(4): 1276–1286.
4. Blazer, DG 3rd, Kishi Y, Maru DM, et al. Pathologic response to preoperative chemotherapy: A new outcome end point after resection of hepatic colorectal metastases. *J Clin Oncol*. 2008;26(33):5344–5351.
5. Koi M, Garcia M, Choi C, et al. Microsatellite alterations with allelic loss at 9p24.2 signify less-aggressive colorectal cancer metastasis. *Gastroenterology*. 2016;150(4):944–955.
6. Mise Y, Zimmitti G, Shindoh J, et al. RAS mutations predict radiologic and pathologic response in patients treated with chemotherapy before resection of colorectal liver metastases. *Ann Surg Oncol*. 2015;22(3):834–842.
7. Rubbia-Brandt L, Giostra E, Brezault C, et al. Importance of histological tumor response assessment in predicting the outcome in patients with colorectal liver metastases treated with neo-adjuvant chemotherapy followed by liver surgery. *Ann Oncol*. 2007;18(2):299–304.
8. Schirripa M, Bergamo F, Cremolini C, et al. BRAF and RAS mutations as prognostic factors in metastatic colorectal cancer patients undergoing liver resection. *Br J Cancer*. 2015;112(12):1921–1928.
9. Foersch S, Sperka T, Lindner C, et al. VEGFR2 signaling prevents colorectal cancer cell senescence to promote tumorigenesis in mice with colitis. *Gastroenterology*. 2015;149(1):177–189, e10.
10. Galon J, Costes A, Sanchez-Cabo F, et al. Type, density, and location of immune cells within human colorectal tumors predict clinical outcome. *Science*. 2006;313(5795):1960–1964.
11. Mlecnik B, Tosolini M, Charoentong P, et al. Biomolecular network reconstruction identifies T-cell homing factors associated with survival in colorectal cancer. *Gastroenterology*. 2010;138(4):1429–1440.
12. Mlecnik B, Tosolini M, Kirilovsky A, et al. Histopathologic-based prognostic factors of colorectal cancers are associated with the state of the local immune reaction. *J Clin Oncol*. 2011;29(6):610–618.

13. Pagès F, Kirilovsky A, Mlecnik B, et al. In situ cytotoxic and memory T cells predict outcome in patients with early-stage colorectal cancer. *J Clin Oncol*. 2009;27(35):5944–5951.
14. Berghoff AS, Fuchs E, Ricken G, et al. Density of tumor-infiltrating lymphocytes correlates with extent of brain edema and overall survival time in patients with brain metastases. *Oncoimmunology*. 2016;5(1):e1.
15. Galon J, Franck P, Marincola FM, et al. Cancer classification using the Immunoscore: A worldwide task force. *J Transl Med*. 2012;10(1):205.
16. Galon J, Mlecnik B, Bindea G, et al. Towards the introduction of the 'Immunoscore' in the classification of malignant tumours. *J Pathol*. 2014; 232(2):199–209.
17. Galon J, Pages F, Marincola FM, et al. The immune score as a new possible approach for the classification of cancer. *J Transl Med*. 2012;10:1.
18. Ferris RL, Galon J. Additional support for the introduction of immune cell quantification in colorectal cancer classification. *J Natl Cancer Inst*. 2016; 108(8):djw033.
19. Eisenhauer EA, Therasse P, Bogaerts J, et al. New response evaluation criteria in solid tumours: Revised RECIST guideline (version 1.1). *Eur J Cancer*. 2009; 45(2):228–247.
20. Altman DG, Lausen B, Sauerbrei W, et al. Dangers of using "optimal" cutpoints in the evaluation of prognostic factors. *J Natl Cancer Inst*. 1994;86(11): 829–835.
21. Gerds TA, Schumacher M. Consistent estimation of the expected Brier score in general survival models with right-censored event times. *Biom J*. 2006; 48(6):1029–1040.
22. Harrell FE Jr, Lee KL, Mark DB. Multivariable prognostic models: Issues in developing models, evaluating assumptions and adequacy, and measuring and reducing errors. *Stat Med*. 1996;15(4):361–387.
23. Heagerty PJ, Zheng Y. Survival model predictive accuracy and ROC curves. *Biometrics*. 2005;61(1):92–105.
24. May S, Hosmer DW. A simplified method of calculating an overall goodness-of-fit test for the Cox proportional hazards model. *Lifetime Data Anal*. 1998; 4(2):109–120.
25. Khan H, Khan N, Ahmad A, et al. Surgical management of metastatic colon cancer: A population-based analysis. *J Geriatr Oncol*. 2015;6(6):446–453.
26. Leonard GD, Brenner B, Kemeny NE. Neoadjuvant chemotherapy before liver resection for patients with unresectable liver metastases from colorectal carcinoma. *J Clin Oncol*. 2005;23(9):2038–2048.
27. Halama N, Michel S, Kloor M, et al. Localization and density of immune cells in the invasive margin of human colorectal cancer liver metastases are prognostic for response to chemotherapy. *Cancer Res*. 2011;71(17):5670–5677.
28. Katz SC, Bamboat ZM, Maker AV, et al. Regulatory T cell infiltration predicts outcome following resection of colorectal cancer liver metastases. *Ann Surg Oncol*. 2013;20(3):946–955.
29. Pugh SA, Harrison RJ, Primrose JN, et al. T cells but not NK cells are associated with a favourable outcome for resected colorectal liver metastases. *BMC Cancer*. 2014;14:180.
30. Tanis E, Julie C, Emile JF, et al. Prognostic impact of immune response in resectable colorectal liver metastases treated by surgery alone or surgery with perioperative FOLFOX in the randomised EORTC study 40983. *Eur J Cancer*. 2015;51(17):2708–2717.
31. Bindea G, Mlecnik B, Tosolini M, et al. Spatiotemporal dynamics of intratumoral immune cells reveal the immune landscape in human cancer. *Immunity*. 2013;39(4):782–795.
32. Naxerova K, Jain RK. Using tumour phylogenetics to identify the roots of metastasis in humans. *Nat Rev Clin Oncol*. 2015;12(5):258–272.
33. Gerlinger M, Rowan AJ, Horswell S, et al. Intratumor heterogeneity and branched evolution revealed by multiregion sequencing. *N Engl J Med*. 2012; 366(10):883–892.
34. Zhang J, Fujimoto J, Zhang J, et al. Intratumor heterogeneity in localized lung adenocarcinomas delineated by multiregion sequencing. *Science*. 2014; 346(6206):256–259.
35. Loes IM, Immervoll H, Sorbye H, et al. Impact of KRAS, BRAF, PIK3CA, TP53 status and intraindividual mutation heterogeneity on outcome after liver resection for colorectal cancer metastases. *Int J Cancer*. 2016;139(3):647–656.
36. Sveen A, Loes IM, Alagaratnam S, et al. Intra-patient inter-metastatic genetic heterogeneity in colorectal cancer as a key determinant of survival after curative liver resection. *PLoS Genet*. 2016;12(7):e1006225.
37. Brunner SM, Kesselring R, Rubner C, et al. Prognosis according to histochemical analysis of liver metastases removed at liver resection. *Br J Surg*. 2014; 101(13):1681–1691.
38. Carrasco J, Gizzi M, Pairet G, et al. Pathological responses after angiogenesis or EGFR inhibitors in metastatic colorectal cancer depend on the chemotherapy backbone. *Br J Cancer*. 2015;113(9):1298–1304.
39. Chun YS, Vauthey JN, Boonsirikamchai P, et al. Association of computed tomography morphologic criteria with pathologic response and survival in patients treated with bevacizumab for colorectal liver metastases. *JAMA*. 2009;302(21):2338–2344.
40. Valentini V, Minsky BD. Tumor regression grading in rectal cancer: Is it time to move forward? *J Clin Oncol*. 2014;32(15):1534–1536.
41. Galon J, Mlecnik B, Marliot F, et al. Validation of the Immunoscore (IM) as a prognostic marker in stage I/II/III colon cancer: Results of a worldwide consortium-based analysis of 1,336 patients. *J Clin Oncol*. 2016;34(15 suppl):3500.
42. Mlecnik B, Bindea G, Angell HK, et al. Integrative analyses of colorectal cancer show Immunoscore is a stronger predictor of patient survival than microsatellite instability. *Immunity*. 2016;44(3):698–711.
43. Schreiber RD, Old LJ, Smyth MJ. Cancer immunoediting: Integrating immunity's roles in cancer suppression and promotion. *Science*. 2011;331(6024):1565–1570.
44. Angell H, Galon J. From the immune contexture to the Immunoscore: The role of prognostic and predictive immune markers in cancer. *Curr Opin Immunol*. 2013;25(2):261–267.
45. Church SE, Galon J. Tumor microenvironment and immunotherapy: The whole picture is better than a glimpse. *Immunity*. 2015;43(4):631–633.
46. Galon J, Angell HK, Bedognetti D, et al. The continuum of cancer immunosurveillance: Prognostic, predictive, and mechanistic signatures. *Immunity*. 2013; 39(1):11–26.
47. Mlecnik B, Bindea G, Angell HK, et al. Functional network pipeline reveals genetic determinants associated with in situ lymphocyte proliferation and survival of cancer patients. *Sci Transl Med*. 2014;6(228):228ra37.
48. Mlecnik B, Bindea G, Kirilovsky A, et al. The tumor microenvironment and Immunoscore are critical determinants of dissemination to distant metastasis. *Sci Transl Med*. 2016;8(327):327ra26.
49. Tosolini M, Kirilovsky A, Mlecnik B, et al. Clinical impact of different classes of infiltrating T cytotoxic and helper cells (Th1, th2, treg, th17) in patients with colorectal cancer. *Cancer Res*. 2011;71(4):1263–1271.
50. Sallusto F, Geginat J, Lanzavecchia A. Central memory and effector memory T cell subsets: Function, generation, and maintenance. *Annu Rev Immunol*. 2004;22:745–763.